Predator Evasion by a Robocrab

Predator Evasion by a Robocrab

Theodoros Stouraitis[1*], Evripidis Gkanias[1*], Jan M. Hemmi[2], and Barbara Webb[1]

[1] Institute of Perception, Action and Behaviour, School of Informatics, University of Edinburgh, Edinburgh, EH8 9AB, UK
bwebb@inf.ed.ac.uk
[2] School of Biological Sciences, University of Western Australia, Crawley, WA 6009, Australia
jan.hemmi@uwa.edu.au

Abstract. We describe the first robot designed to emulate specific perceptual and motor capabilities of the fiddler crab. An omnidirectional robot platform uses onboard computation to process images from a 360° camera view, filtering it through a biological model of the crab's ommatidia layout, extracting potential 'predator' cues, and executing an evasion response that also depends on contextual information. We show that, as for real crabs, multiple cues are needed for effective escape in different predator-prey scenarios.

1 Introduction

Fiddler crabs are a semi-terrestrial marine species of crab which use visual information to make behavioural decisions such as escaping from predators, selecting

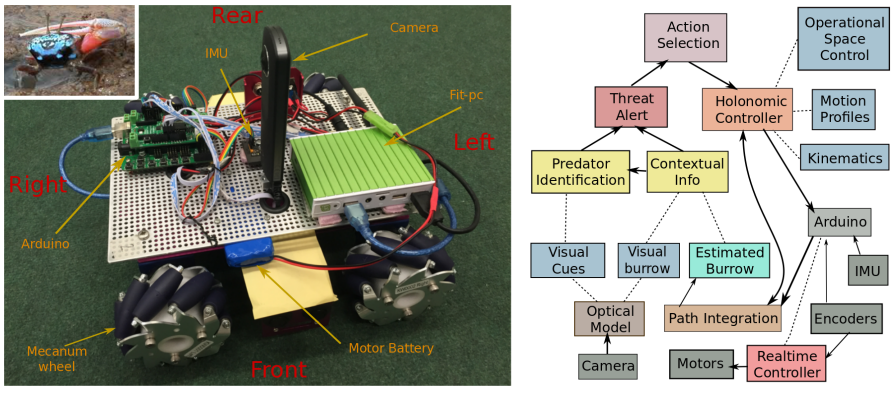

(a) (b)

Fig. 1: (a) The Robocrab (inset: a real crab). (b) System schematic. Arrows: communication of data; dashed lines: hierarchical component relations.

*Theodoros Stouraitis and Evripidis Gkanias contributed equally to this work and jointly assert first authorship.

mates, signalling conspecifics and detecting their burrows [5, 6, 16, 21]. We explore the mechanisms of crab behaviour using a biorobotic approach (Fig. 1).

Courtship and burrow defence are regulated from the stimuli detected below the horizon, while the stimuli for initiating the evasion behaviour are detected above the horizon [6]. This paper focuses on the evasion behaviour of fiddler crabs, as its visuomotor characteristics, response stages and context dependence have been extensively studied [5].

An important characteristic of fiddler crabs is their ability to move in any direction while maintaining a fixed orientation or rotating around their centre of mass independently of translation. This allows them to escape rapidly from a potential threat independently of their pose. Another striking feature is their two panoramic compound eyes, located on eyestalks on the front part of the carapace, each with a 360° view. The eyes are composed from a large number of ommatidia in a particular layout, specialised for detection of behaviourally relevant cues [15], despite the low resolution [5]. In addition, the fact that crabs live on mud flats simplifies the identification the visual horizon and alignment of the eye equator to it [21].

The initiation of the evasion response depends not only on the location of the stimuli above the horizon but on additional cues and context [3]. The response itself can also differ. When a fiddler crab identifies a threatening stimulus but does not have a burrow, it first freezes, then runs in the opposite direction to the stimulus and rotates around its centre of mass to place the threatening stimulus on one of its sides [7]. On the other hand, burrow-holder fiddler crabs always run towards their burrow under the presence of any threatening stimulus [2], and will then pause again outside the burrow before making a descent.

In the following sections we describe the hardware choices, then the implementation of motion control, path integration, visual processing and behavioural intelligence. This is followed by the results of experiments on the evasion response of the robot, using the same paradigm as has been used for crabs. We discuss the conclusions that can be drawn and the plans for future work.

2 Methods

Robot Platform Fiddler crabs have complex legged actuation, but for the purposes of mimicking escape, the crucial feature is their ability to execute omnidirectional motions on a 2D plane (the mud flat), described by a 3D motion vector (x, y, θ), where x and y define the position in the 2D space and θ the orientation. Thus, the robot platform used is omnidirectional, utilising Mecanum wheels, in which the sideways forces exerted by the rollers attached to the wheels can be used in combination to obtain any direction of motion (see section 2). Each wheel is actuated by a DC motor. The actual size of the robot is x10 factor larger than the real fiddler crab.

This work was in part supported by an Australian Research Council (ARC) Discovery Grant (DP160102658).

Sensory systems Each motor is equipped with an optical encoder used for odometry, equivalent to propriceptive input for leg motion in the crab. We added an IMU (inertia measurement unit) to replicate the statocyst organ of the fiddler crabs [14]. The robot is equipped with a Ricoh Theta S camera to imitate the eyestalks of the fiddler crabs, and provide a 360° field of view.

Electronics, Processing and Communications The robot platform includes a custom Arduino board (Duemilanove) and the respective I/O expansion shield with interfaces to the sensors and the motors, which is used for real-time processing. The main processing unit is a fanless lightweight (250 grams) PC which is used for image processing on the fly, on-board motion control and decision making processes. The PC and Arduino communicate via serial port, through an asynchronous communication interface.

Motion controller Fig. 2b summarises the method implemented to enable a pose command in the operational space of the robot x, y, θ to result in the corresponding movement of the robot base, following the methods in [13, 18, 19]. Every time a new pose command is received by the tracker, the motion profile module is called to provide a sinusoidal motion profile to implicitly control the accelerations of the system. The output is the interpolated substeps for each of the three dimensions x, y, θ. Next, the complete trajectory is tracked utilising the operational space controller which is running at 15 Hz with a fixed duty cycle for each substep. This uses three PD controllers one for each dimension x, y and θ to reach any target in the 3D space, plus a feedforward term to reduce the reaction time. This produces the desired robot velocities $\dot{x}, \dot{y}, \dot{\theta}$ which then need

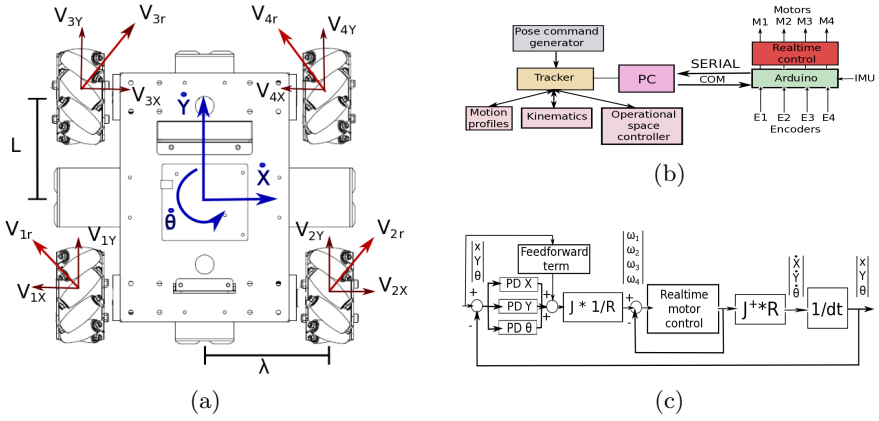

Fig. 2: (a) Robot frame, operation space velocities and linear velocities at the mounting points of the wheels, due to angular velocities of the wheels. (b) System software architecture. (c) Control structure including operational space and realtime controller.

to be transformed to motor/wheel velocities $\omega 1, \omega 2, \omega 3, \omega 4$ through kinematic modelling of the robot (Fig. 2a). These are sent to the Arduino, on which the realtime controller realises the specified motor angular velocities on the motors using 200Hz PID control for each wheel.

Path integration Fiddler crabs use path integration to maintain an accurate estimate of their position relative to their burrow while foraging. In [8] and [9] Layne claims that crabs can accurately path integrate solely due to their leg proprioceptor sensors. However, crabs also possess an advanced statocyst organ that is capable of sensing accurately linear and angular accelerations [14]. Hence, we decided to utilise both the wheel encoders as well as an IMU to localise the Robocrab based on the work presented in [1], [10] and [20].

Utilising motors' optical encoders and inverse kinematics, the Robocrab's velocities in the 3D space x, y, θ are estimated. Using acceleration and orientation information from the Inertia Measurement Unit (IMU), a second estimate of Robocrab's velocities is obtained. The two estimates are fused with a complementary filter to obtain a robust estimate of Robocrab's velocities, that is integrated to get the pose of the robot relative to burrow.

Modelling the compound eye The spatial distribution of ommatidia in the compound eye is described by the sampling resolution and every ommatidium has its own optical resolution (i.e. receptive field). We use the model from [15] (supplied to us by the authors) which describes the optical resolution using a Gaussian distribution for each ommatidium, while for the sampling resolution a combination of inverse sine functions is used. This model consists of $7,971$ ommatidia positions in spherical coordinates (elevation, azimuth and radius). To create our twin-eye model we just drop the samples from the medial zone, duplicate the lateral zone, and invert the y axis to create the half-right eye.

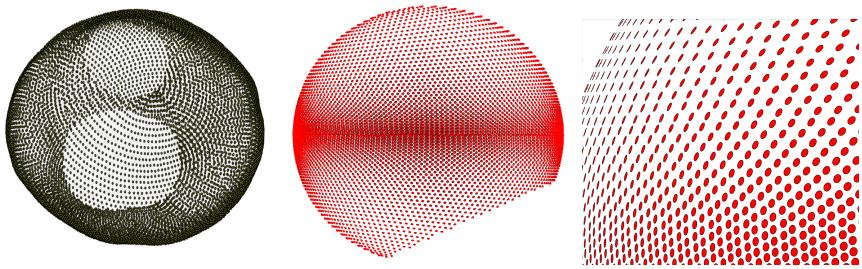

(a) (b) (c)

Fig. 3: Sampling and optical resolution of the twin-eye model. (a) represents the 3D model of the twin-eye sampling resolution. In (b) we represent the optical resolution of the left half-eye using Gaussian contours on the $Y - Z$ axes. This is more visible in (c), where we plot a closer view of it.

Fig. 4: A fully panoramic 360° crab's view image, created using Voronoi diagrams and the twin-eye sampling resolution model.

Finally, we merge the two half-eyes to create the twin-eye of Fig. 3a. This model has $9,740$ ommatidia in total, $4,870$ for each eye. To reduce the compution cost of applying a Gaussian filter for each ommaditium, we instead filter the image before sampling from it using two different filters: for the central pixels we use *Gaussian blurring* to incorporate information from all the adjacent pixels of every sample; and for the peripheral samples we use *rotational blurring* to imitate the Gaussian blurring on the fisheye-image. To visualise the result we use Voronoi diagrams to fill sets of pixels with the colour of their corresponding ommatidia (Fig. 4).

Visual cue extraction Fiddler crabs typically live in areas with open, clear skies, hence a predator above the horizon, typically a bird, can be detected by its high contrast against the bright sky [21]. In the lab the segmentation of the artificial predator and burrow from the cluttered background is achieved by using a distinctive colour for these objects and utilising a simple colour filter from OpenCV as shown in Fig. 5. Such filtering provides a noisy segmentation signal, similar to a natural one. A Jacobian matrix V_j maps the pixel space to the ommatidia space. The set of activated ommatidia is described as a 2D contour within the 3D manifold shaped by the 3D placement of the ommatidia in space.

First, we assume that any detected object below the horizon level is the burrow and only objects above the horizon could be a potential predator. Based on the findings on [4], [16] and [21] a set of visual cues that are assumed to be used by the fiddler crabs in order to identify whether the detected object is a predator or not are extracted:

- Ommatidia number : Number of activated ommatidia.
- Elevation : The elevation of the centroid of the ommatidia region.
- Azimuth : The azimuth of the centroid of the ommatidia region.
- Elevation velocity : Angular vertical velocity of the ommatidia region [16].
- Azimuth velocity : Angular horizontal velocity of the ommatidia region [16].

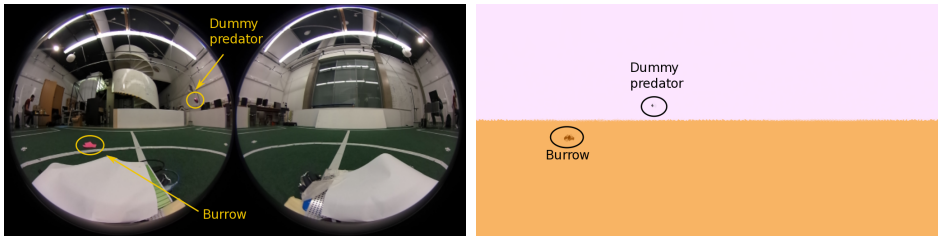

(a) (b)

Fig. 5: (a) Captured fisheye images of a cluttered environment, with pink burrow and predator. (b) Stitched panoramic image after it has been colour filtered and passed through the optics of the eye model.

- Looming : The rate the activated ommatidia region grows [11].
- Flickering : The rate of activation and deactivation of the ommatidia region within a window of x frames [16].

Behavioural intelligence In Fig. 1b we provide a schematic representation of the overall system, with the following behavioural intelligence components:

Predator Identification: First, it is necessary to identify the predator given the visual cues. In [3], [4], [16] and [21] biologists present quantitative results that relate the triggering of the evasion with the respective set of visual cues. Consequently, for the robot, the predator identification block uses some of the visual cues and if one or more of these quantities exceed its respective upper threshold value, then the detected object is classified as predator.

Contextual Information: In [12] and [17] it has been demonstrated that fiddler crabs and other species of crabs are able to incorporate contextual information in their decision making scheme and alter their actions according to them. The contextual submodule for the Robocrab tracks whether it has a burrow or not, which will determine the direction of the evasive response; and whether the burrow location information should be taken from the path integration module or the visual detection of the burrow.

Threat Alert: In [2], fiddler crabs are shown to evaluate their risk level and compare it with the cost of an evasion action to decide whether they should perform an action or not. The threat alert module is obtains the contextual information and predator characteristics from the two previously introduced submodules and updates the threshold limits according to the risk level in a inverse proportional fashion. In our current implementation the risk level is a linear function of the distance to the burrow. Additionally, the threat alert submodule declares whether a threat is present or not and initiates the evasion response.

Action Selection: The action sets are basically separated into two layers. The first distinction is between the burrow-holder and non-burrow holder, determined by contextual information. The second layer includes actions corresponding to the stages of the evasion response as in section 1. Thus, depending on Robocrab's

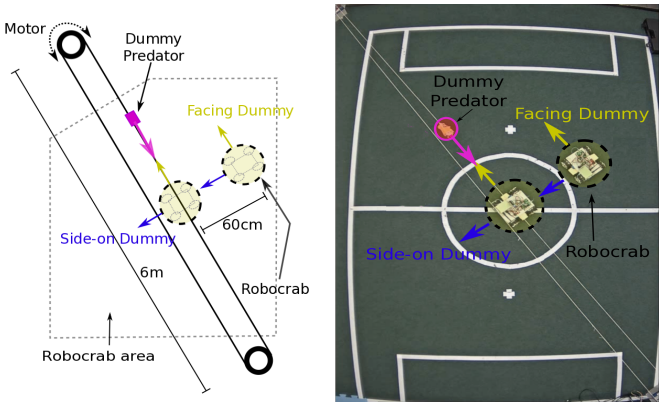

(a) (b)

Fig. 6: Sketch (a) and the original top-view representations (b) of the experimental set-up, illustrating the four sets of experiments with the robot being placed under and off track and facing the dummy or side-on the dummy.

evasion stage, the respective action is selected. In a burrow-holder scenario, the action selection module coordinates the motion control with the localisation and the visual information of the burrow location to return to its burrow. For a non-burrow holder, it coordinates the motion control module with the visual based predator location to run away from the threat.

3 Results

Experimental methods To evaluate the performance of the robot we run a set of experiments similar to those reported for crabs in [3], where a dummy predator (a sphere pulled along a straight track, see Fig. 6) is used to stimulate and evasion response in a stationary crab. We track the evolution of the relevant visual cues preceding the moment in which the robot reacts to examine which cue is most effective for triggering the response.

In the first two scenarios we look at the 'home-run' response, and in the second at the 'burrow-descent' response, which in the crab and our model involves different visual cues. Specifically, we set the thresholds for the home-run stage at 4 activated ommatidia, $0.020\,rad\,s^{-1}$ horizontal or $0.018\,rad\,s^{-1}$ vertical velocity; and for burrow-descent at 20 activated ommatidia, or a looming rate of 1 (doubling the size in one frame) with a minimum of 5 activated ommatidia. The thresholds were tuned based on preliminary experiments to obtain similar behaviour to fiddler crabs and they are indicated by the horizontal-dashed line in the figures.

For the home-run, we test the robot from two positions, either $60\,cm$ offset from the track of the dummy with the dummy moving at a constant speed of $62\,cm\,s^{-1}$, or directly under the track of the dummy, with a speed of $47\,cm\,s^{-1}$,

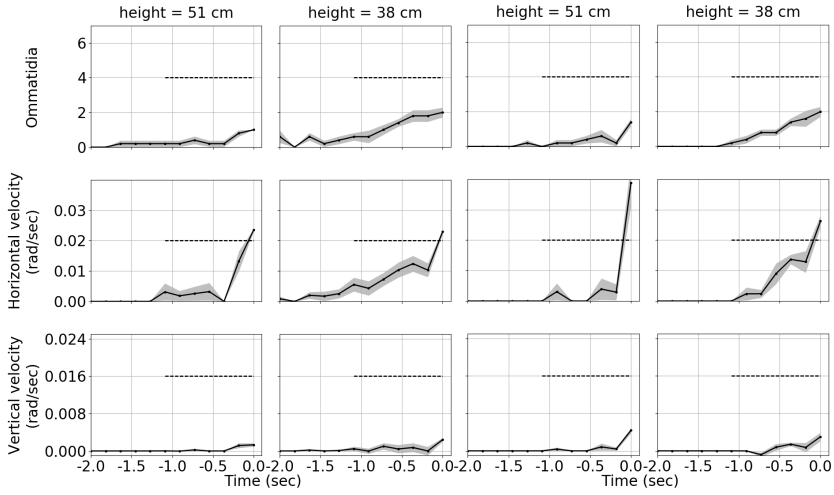

(a) facing (b) side-on

Fig. 7: Visual cue evolution during the 2 *sec* preceding a response during off-track home-run experiments with two heights and directions of the dummy predator.

as in [3]. In each case we test with the robot either facing towards the dummy's approach direction or side-on, and at two different heights (38 *cm* and 51 *cm*) of the stimulus. Notice that the height of centre of the camera lens mounted on the robot is at 26 *cm* distance from the ground. This produces a total of eight test conditions, and we run 5 trials for each condition. For the burrow-descent, we test with the robot under the track and the dummy at a lower height (32 *cm*), again facing or side-on to the predator, and with two different approach speeds, $62\,cm\,s^{-1}$ or $15\,cm\,s^{-1}$. This produces 4 further conditions for each of which we again run 5 trials.

Home-run, offset from the predator track This simulates a scenario in which a predator flies along the horizon passing by the crab. When the robot is side-on to the dummy, for both heights of the dummy, we see that the triggering is caused by the horizontal velocity (see Fig. 7b). A higher horizontal velocity is obtained for the higher dummy, leading to a more reliable reaction when the dummy is more distant (see Fig. 10). This could be a result of the limited number of ommatidia available for the higher elevations of the eye model. The vertical velocity does not provide any useful information, and at the reaction frame, the number of activated ommatidia is only around 2 for the lower dummy, and 1 for the higher dummy, i.e., well below threshold. When the robot is facing the predator approach direction, we do not see much difference, with the horizontal velocity still providing the most information (Fig. 7a). The robot is able to track

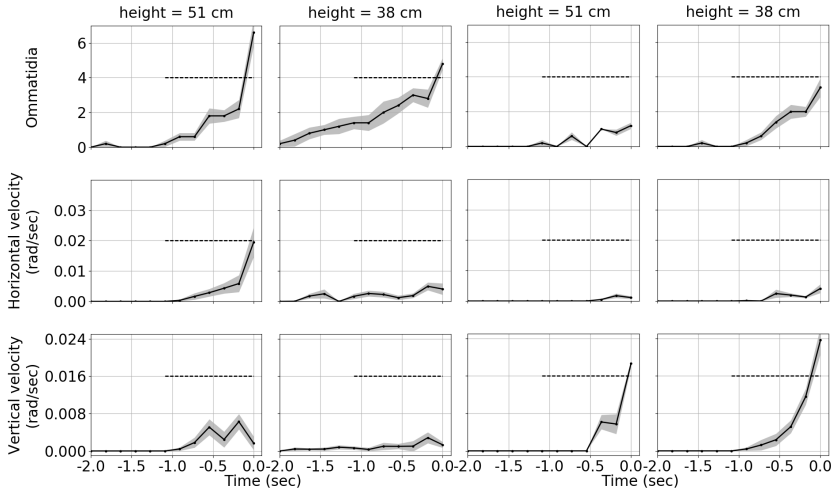

(a) facing (b) side-on

Fig. 8: Visual cue evolution during the 2 *sec* preceding a response during under-track home-run experiments with two heights and directions of the dummy predator.

the dummy from a longer distance/time due to the higher sampling resolution in the frontal vs. lateral field. However, it reacts when the dummy is at a shorter distance (Fig. 10) and the higher dummy triggers a later reaction.

Home-run, under the predator track This case resembles a predator flying directly above a crab. With the robot side-on to the predator, at both dummy heights, the vertical velocity triggers the escape, while the horizontal velocity does not provide useful information. The ommatidia values are similar to the off-track experiments with a difference in the lower height scenario, where the average number of ommatidia activated at the reaction frame is nearer to the threshold. In Fig. 10 we can see that the robot waits for the dummy to come closer before it reacts, but the uncertainty is greater for the higher dummy, with some reactions occurring only when the dummy is right above the robot.

By contrast, when facing the dummy the number of activated ommatidia is the visual cue which triggers the evasion (see Fig. 8a). From the figures, it is clear that a lower track-height allows the robot to track the dummy for longer time and more consistently. However, compared to the side-on under-track experiment, the robot reacts earlier regarding the distance from the dummy (see Fig. 10). The cause of this unexpected result is the fact that the frontal area of our eye's model is the location where the merging of the two eyes happens. When we merge the two eyes an object in the environment of the robot could be seen by both half-eyes

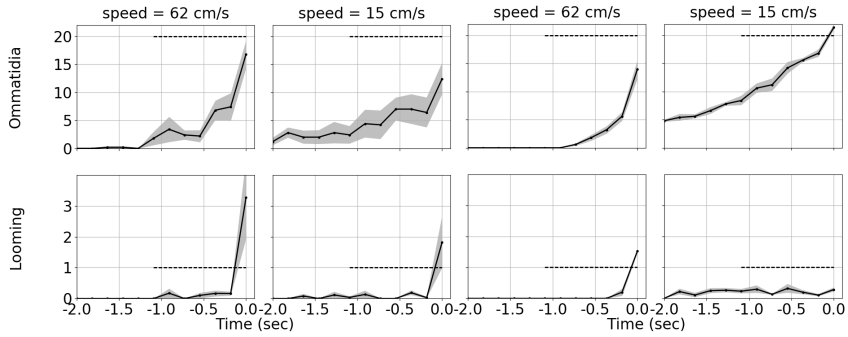

(a) facing (b) side-on

Fig. 9: Visual cue evolution during the 2 *sec* preceding a burrow descent response, with two speeds and directions of the dummy predator.

depending on its distance from the robot. This could cause an abnormally large ommatidia-blob (number of ommatidia activated) or excessively high horizontal velocity, which could be result of trading the activated ommatidia from the one eye to the other in almost each subsequent frame. This effect could duplicate the number of activated ommatidia and increase the perceived horizontal velocity. In the higher track scenario this issue is even more apparent, as the ommatidia-blob is smaller and therefore its detection is less consistent. However, these artefacts appear due limitations of the twin-eye model, which were a trade-off to use only one 360° camera as described in section 2.

Burrow descent As described in the methods, we finally examined the evolution of visual cues relative to the 'burrow-descent' stage of the crab's behaviour. This assumes the crab has reached its burrow and now requires a stronger threat to make the costly move of entering it, and as described in the experimental methods, relies on different cues. When the robot is side-on to the predator, Fig.

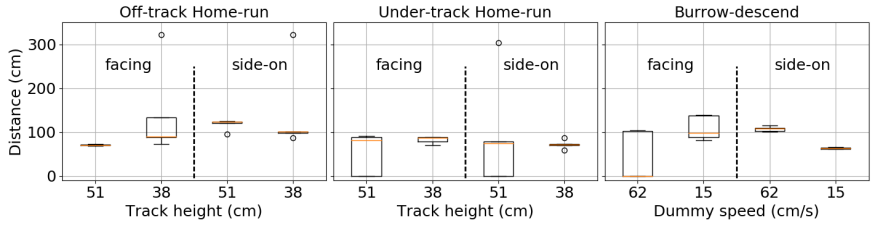

Fig. 10: The distance of the dummy from the robot at the reaction frame for every experimental scenario.

9b illustrates that in a fast dummy attack the robot evasion is caused by the looming, while in a slow one the number of activated ommatidia will trigger the behaviour when the dummy is close enough to the robot. Following the experiments in [11], this could be a reasonable reaction scenario. In Fig. 10 we can see that the robot reacts in a greater distance from the predator in a fast attack rather than a slow one.

On the other hand, aligning the frontal axis to the track gives unexpected results. As for the under-track experiments, the looming and the activated ommatidia numberare over-activated because of the twin-eye stitching. Fig. 9a shows that slow dummies activate the looming, which is unrealistic, but can be explained if the robot sees the dummy with one eye in one time-step and with both eyes in the next. Additionally, Fig. 10 shows that there is great uncertainty about the reaction distance, while in the fast-dummy scenario the robot has very limited time to react due to the above confusion, leading to a very late response.

4 Discussion

We have demonstrated for the first time a robot design, the Robocrab, that is a suitable platform to explore hypotheses about the evasion behaviour of real crabs. It perceives the world through the same filter as a crab eye, can perform omnidirectional movement, and can be tested under comparable experimental conditions. In this paper we showed how this allowed us to test the effectiveness of different visual cues to initiate the evasion response. The behavioural intelligence framework allows this response to be modulated by the presence or absence of a burrow, and the estimated distance of the burrow, based on path integration. Qualitative results of the evasion behaviour are demonstrated with videos.

We plan to further explore the visual experience of the Robocrab during escape. Without a burrow, it attempts to move away from the predator; with a burrow, it attempts to return to the estimated location. This raises the interesting issue of whether and how crabs may compensate for their own self motion while continuing to assess the visual threat, and whether the initial freeze stage is important in its decision-making. In practice, it has proved difficult to obtain path integration of comparable accuracy to the crab so this will be our future focus. We are also interested to use this system to explore the learning observed in crabs to repeated threatening stimuli, and ultimately to understand the underlying neural processes of this complex, coordinated behaviour.

References

1. J. Borenstein and L. Feng. Gyrodometry: A new method for combining data from gyros and odometry in mobile robots. In *Robotics and Automation, IEEE 1996.*, volume 1, pages 423–428.
2. J. M Hemmi. Predator avoidance in fiddler crabs: 1. escape decisions in relation to the risk of predation. *Animal Behaviour*, 69(3):603–614, 2005.

www.youtube.com/playlist?list=PLwwwvIsWO7M_SbmdCKl1siL9ajmSHzohw

3. J. M Hemmi. Predator avoidance in fiddler crabs: 2. the visual cues. *Animal behaviour*, 69(3):615–625, 2005.
4. J. M Hemmi and A. Pfeil. A multi-stage anti-predator response increases information on predation risk. *The Journal of experimental biology*, 213(9):1484–1489, 2010.
5. J. M Hemmi and D. Tomsic. The neuroethology of escape in crabs: from sensory ecology to neurons and back. *Current opinion in neurobiology*, 22(2):194–200, 2012.
6. M. Land and J. Layne. The visual control of behaviour in fiddler crabs: I. resolution, thresholds and the role of the horizon. *Journal of Comparative Physiology A*, 177(1):81–90, 1995.
7. M. Land and J. Layne. The visual control of behaviour in fiddler crabs: II. tracking control systems in courtship and defence. *Journal of Comparative Physiology A*, 177(1):91–103, 1995.
8. J. Layne, W J P. Barnes, and L. MJ Duncan. Mechanisms of homing in the fiddler crab uca rapax 1. spatial and temporal characteristics of a system of small-scale navigation. *Journal of experimental biology*, 206(24):4413–4423, 2003.
9. J. Layne, W J P. Barnes, and L. MJ Duncan. Mechanisms of homing in the fiddler crab uca rapax 2. information sources and frame of reference for a path integration system. *Journal of Experimental Biology*, 206(24):4425–4442, 2003.
10. K. Nagatani, S. Tachibana, M. Sofne, and Y. Tanaka. Improvement of odometry for omnidirectional vehicle using optical flow information. In *IROS 2000. Proceedings. 2000 IEEE/RSJ International Conference on*, volume 1, pages 468–473.
11. D. Oliva and D. Tomsic. Visuo-motor transformations involved in the escape response to looming stimuli in the crab neohelice (= chasmagnathus) granulata. *Journal of Experimental Biology*, 215(19):3488–3500, 2012.
12. C. A. Raderschall, R. D Magrath, and J. M Hemmi. Habituation under natural conditions: model predators are distinguished by approach direction. *The Journal of experimental biology*, 214(24):4209–4216, 2011.
13. R. Rojas and A. G. Förster. Holonomic control of a robot with an omnidirectional drive. *KI-Künstliche Intelligenz*, 20(2):12–17, 2006.
14. DC Sandeman. Dynamic receptors in the statocysts of crabs. *Fortschritte der Zoologie*, 23(1):185, 1975.
15. J. Smolka and J. M Hemmi. Topography of vision and behaviour. *Journal of Experimental Biology*, 212(21):3522–3532, 2009.
16. J. Smolka, J. Zeil, and J. M Hemmi. Natural visual cues eliciting predator avoidance in fiddler crabs. *Proceedings of the Royal Society of London B: Biological Sciences*, 278(1724):3584–3592, 2011.
17. D. Tomsic, M. B. de Astrada, J. Sztarker, and H. Maldonado. Behavioral and neuronal attributes of short-and long-term habituation in the crab chasmagnathus. *Neurobiology of learning and memory*, 92(2):176–182, 2009.
18. C. Tsai, F. Tai, and Y. Lee. Motion controller design and embedded realization for mecanum wheeled omnidirectional robots. In *Intelligent Control and Automation (WCICA), 2011 9th World Congress on*, pages 546–551. IEEE, 2011.
19. P. Viboonchaicheep, A. Shimada, and Y. Kosaka. Position rectification control for mecanum wheeled omni-directional vehicles. In *Industrial Electronics Society, 2003. IECON. The 29th Annual Conference of the IEEE*, volume 1, pages 854–859.
20. J. Yi, J. Zhang, D. Song, and S. Jayasuriya. Imu-based localization and slip estimation for skid-steered mobile robots. In *IROS 2007. IEEE/RSJ International Conference on*, pages 2845–2850. IEEE, 2007.
21. J. Zeil and J. M Hemmi. The visual ecology of fiddler crabs. *Journal of Comparative Physiology A*, 192(1):1–25, 2006.